

Polar-bulge galaxies

V.P. Reshetnikov¹, S.S. Savchenko¹, A.V. Mosenkov^{1,2,3}, N.Ya. Sotnikova¹, D.V. Bizyaev^{4,5}

¹ St.Petersburg State University, Universitetskii pr. 28, St.Petersburg, 198504 Russia

² Sterrenkundig Observatorium, Universiteit Gent, Belgium

³ Central (Pulkovo) Astronomical Observatory of RAS, Russia

⁴ Apache Point Observatory and New Mexico State University, USA

⁵ Sternberg Astronomical Institute, Moscow State University, Russia

Based on SDSS data, we have selected a sample of nine edge-on spiral galaxies with bulges whose major axes show a high inclination to the disk plane. Such objects are called polar-bulge galaxies. They are similar in their morphology to polar-ring galaxies, but the central objects in them have small size and low luminosity. We have performed a photometric analysis of the galaxies in the g and r bands and determined the main characteristics of their bulges and disks. We show that the disks of such galaxies are typical for the disks of spiral galaxies of late morphological types. The integrated characteristics of their bulges are similar to the parameters of normal bulges. The stellar disks of polar-bulge galaxies often show large-scale warps, which can be explained by their interaction with neighboring galaxies or external accretion from outside.

Keywords: galaxies, bulges, interacting galaxies, morphology

1. Introduction

The bulge is one of the main subsystems of spiral galaxies. Bulges distinguish from the other galactic subsystems (disks, bars, spiral arms, etc.) by their brightness distribution, shape, stellar population, the pattern of stellar motion, and other characteristics. For a long time the bulges were considered as a kind of small elliptical galaxies surrounded by stellar disks. In the last couple of decades this simplified picture has changed to a more complex one: it turned out that the bulges are not a homogeneous type of objects. They break up into at least two different groups: the classical bulges that resemble elliptical galaxies in many respects (see, e.g., Renzini, 1999) and the pseudo-bulges that are closer to galactic disks in a number of characteristics (Kormendy and Kennicutt 2004; Kormendy 2015). Athanassoula (2005) introduced the third type, boxy/peanut bulges, that are actually edge-on bars. The situation is further complicated by the fact that different types of bulges can co-exist in the same galaxy (see, e.g., Erwin et al. 2015).

In this paper we consider yet another type of bulges, the bulges whose apparent major axis is

highly inclined to the galactic midplane. The objects with such bulges are similar in their morphology to the polar-ring galaxies whose polar component dominates in luminosity. Corsini et al. (2012) called such bulges *polar*. The polar bulges are extremely rare. In a recent review devoted to the shape of galactic bulges, Méndez-Abreu (2015) mentions only three such galaxies: NGC 4698 (Bertola et al. 1999; Corsini et al. 2012), NGC 4672 (Sarzi et al. 2000), and UGC 10043 (Matthews and de Grijs 2004). One of the reasons for the small number of known polar bulges is that they can be identified only in the case where the galactic disk is close to the edge-on orientation to the line of sight and therefore, the bulge inclination to the disk plane can be easily detected. If this is not the case, then the bulge looks like a bar and does not attract the attention of researchers.

Given the small number of known objects, the systematics of properties and the origin of the polar bulges remain puzzles. In two of the three galaxies (NGC 4698 and NGC 4672) the morphologically decoupled bulges are known to be related to the kinematically decoupled subsystems in their cores

that rotate almost orthogonally to the galactic disks (Bertola et al. 1999; Sarzi et al. 2000). No kinematically decoupled core was detected in UGC 10043 (Matthews and de Grijs 2004), although as the authors note, this could be hindered by the limited spatial resolution of the spectra they used and by the powerful absorption stripe that shields the core.

The existence of kinematically and morphologically decoupled structures in galaxies is usually associated with a “secondary” event in their history. To explain the formation of polar bulges, Matthews and de Grijs (2004) considered three possible “secondary” events: the capture of a disk by a pre-existing “naked” bulge (this scenario resembles the formation of polar-ring galaxies with the external accretion; Reshetnikov and Sotnikova 1997); the capture of a small elliptical galaxy by a spiral galaxy (this mechanism resembles the formation of collisional rings, but the relative velocity of the galaxies must be small; Appleton and Struck-Marcell 1996); and merging of two disk galaxies (Bekki 1998). Qualitatively, all these scenarios are capable of describing a number of peculiarities of polar-bulge galaxies, and extensive observational data are needed to choose between them. First of all, it is necessary to increase the sample of known objects of this type and to perform their detailed observational study and simulations.

In this paper, we present a small sample of new candidates to the polar-bulge galaxies and some results of their photometric analysis. All numerical values in the paper are given for the cosmological model with the Hubble constant of $70 \text{ km s}^{-1} \text{ Mpc}^{-1}$ and $\Omega_m = 0.3$, $\Omega_\Lambda = 0.7$.

2. The sample of polar-bulge galaxies and their analysis

2.1. The sample of galaxies

In order to search for galaxies with morphologically decoupled bulges we examined images of galaxies from the EGIS (Edge-on Galaxies In SDSS) catalog (Bizyaev et al. 2014), which includes almost six thousand edge-on galaxies. Our examination revealed more than twenty objects whose bulges visually appeared elongated along the galaxy minor axis. As the next step, we performed a photometric decomposition of the images of all selected galaxies and estimated parameters of the disks and bulges, including their apparent flattening and position angles of the apparent major axes (see the next section for the details of our analysis). Our final sample of nine candidates to

the polar-bulge galaxies includes only those objects whose bulges in the g and r bands showed an apparent flattening $b/a < 0.9$, while the difference between the position angles of the major axes for the disks and bulges exceeded 30° . The accuracy of the model parameters (see below) does not allow us to reliably judge whether the bulges with $b/a \geq 0.9$ can belong to the polar ones.

Table 1 is based of the SDSS¹ and NED² data, and summarizes the main characteristics of the final sample of the polar-bulge galaxies. Their r -band contour maps are shown in Fig. 1. As it can be seen from the table, two galaxies (#1 and #5) were previously included in the catalog of candidates to the polar-ring galaxies (SPRC; Moiseev et al. 2011) due to their unusual morphology. The galaxy UGC 10043 (no. 7 in Table 1) was studied by Matthews and de Grijs (2004) (see the Introduction).

2.2. Photometric analysis

To determine the photometric and structural parameters of the considered galaxies, we decomposed their g - and r -band images within the framework of the two-component “bulge + disk” model. The galaxy images were taken from the SDSS archive (SDSS DR12; see Alam et al. 2015).

To describe the surface brightness distribution in the bulge, we used the Sersic (1963) law:

$$I(r) = I_{0,b} \exp \left[-\nu_n \left(\frac{r}{r_e} \right)^{\frac{1}{n}} \right], \quad (1)$$

where $I_{0,b}$, r_e and n are the central surface brightness, effective radius, and Sersic parameter, respectively; ν_n is an n -dependent constant chosen in such a way that a half of the total bulge luminosity was encompassed within the r_e . The standard model of an edge-on disk (van der Kruit and Searle 1981) was used as the disk model:

$$I(r, z) = I_{0,d} \left(\frac{r}{h} \right) K_1 \left(\frac{r}{h} \right) \text{sech}^2 \left(\frac{z}{z_0} \right), \quad (2)$$

where $I_{0,d}$, h and z_0 are the central surface brightness, radial scale length and vertical scale height of the disk, and K_1 is a modified first-order Bessel function.

The decomposition, i.e., the search for optimal parameters that ensured the minimal residual between

¹ <http://www.sdss.org>

² <http://ned.ipac.caltech.edu>

Table 1. Candidates for the polar-bulge galaxies

#	SDSS name	Alternative name	Type	r (mag)	z
1	SDSS J015858.39-002923.2	SPRC-77		17.53	0.08099
2	J095346.69+351456.8			16.62	0.03928
3	J102343.67+421917.9			15.59	0.04611
4	J124331.21-142015.8	FGC 1494, RFGC 2365	Sc	16.72	
5	J133904.58+020949.5	UGC 8634, FGC 1649, RFGC 2619, SPRC-42	Sb	15.10	0.02337
6	J151223.37+013823.9			16.58	0.02850
7	J154841.10+215208.7	UGC 10043, FGC 1953, RFGC 3043	Sbc	14.34	0.00721
8	J160028.24+143201.2			15.96	0.03413
9	J222006.54+253621.0			16.96	0.04164

the model and observations, was performed according to the following scheme. At the preliminary stage, the preparation of images was made, including the image rotation in such a way that the galaxy major axis was oriented along the x-axis of the image (the method from Martin-Navarro et al. (2012) was used to find the galaxy position angle), the cropping of the images, and the masking of background objects and dust lanes in the galaxies (if they were visible). At the next stage we obtained the first approximation of the galaxy model using the Differential Evolution algorithm from the "Imfit" package (Erwin 2015). The advantage of this algorithm is that it does not require specific initial conditions for the optimization process and only the range of possible parameters is needed for its operation. The parameters obtained in this way were then improved using the gradient descent algorithm implemented in the "galfit" package (Peng et al. 2010). The output parameters from the "galfit" were assumed as the final galaxy model parameters.

Since the galaxies in our sample have rather small angular sizes, atmospheric seeing strongly affects the parameters being determined (e.g., Trujillo et al. 2001). To compensate for this effect, we convolved the photometric model with the point spread function (PSF) simulating atmospheric seeing and compared the convolved model with the observed image. Here, we used the Moffat function (Moffat 1969) as the PSF. We determined the parameters of the Moffat function by fitting isolated field stars. As a rule, there were 10 - 20 such PSF stars in the field of each galaxy, which allowed us to reliably determine the PSF pa-

rameters and to estimate the dispersion of these parameters.

To estimate the errors of the decomposition results, we performed Monte Carlo simulations by assuming that the main sources of errors were the image noise and the discrepancy between the model and real PSFs. For each galaxy, we constructed a model corresponding to the parameters determined during the decomposition, convolved it with the observed PSF, and added noise whose value corresponded to the real parameters. The PSF parameters differed from their true values according to a normal law with a dispersion equal to the dispersion of the parameters of individual PSF stars obtained at the PSF construction stage. For each galaxy, we repeated the decomposition procedure 250 times and obtained the mean values and the uncertainties of the decomposition parameters.

The mean difference between the total magnitudes (defined as the sum of the model bulge and disk) and the *modelMag* magnitudes from the SDSS is $-0^m.37 \pm 0^m.29$ in the g band and $-0^m.23 \pm 0^m.25$ in the r band. If we take into account the fact that the SDSS photometric data are marked as unreliable for four galaxies, then the agreement becomes better for the remaining five galaxies: $-0^m.21 \pm 0^m.10$ and $-0^m.10 \pm 0^m.14$ in the same bands. In the subsequent discussion, we use the results of our photometry.

The results of our photometric decomposition of the galaxies from the sample in the r band are shown in Table 2. For each object, the first row of the table gives the measured parameter and the second

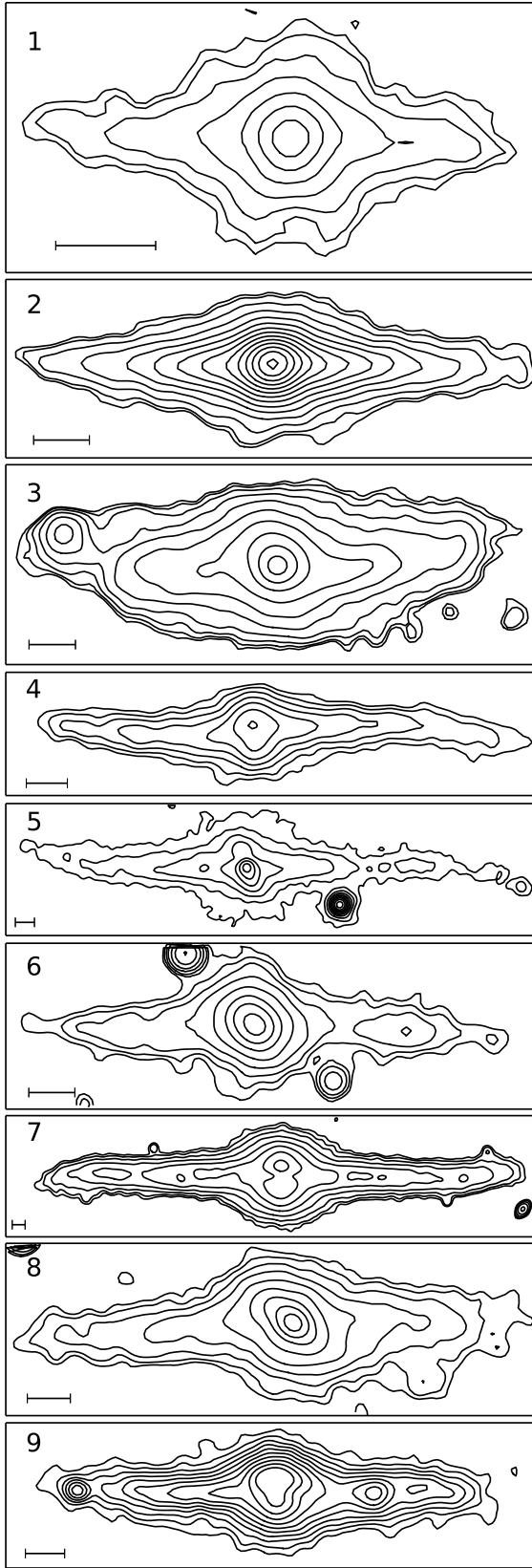


Fig. 1. The r -band contour maps of the galaxies with morphologically decoupled bulges. The contours were selected in a way to highlight the global structure of each galaxy. The galaxy number from Table 1 is indicated in the upper left corner of each panel. The length of the bar in the lower left corner is 10 arcsec.

row gives the measurement uncertainty of this parameter estimated as described above. The first column in Table 2 contains the galaxy number according to Table 1. The next four columns present the bulge parameters: the effective surface brightness, effective radius, Sersic index and apparent flattening. The next columns show the following characteristics of the galactic disks: the observed central surface brightness, exponential scale length, and vertical scale height of the brightness distribution. The observed difference between the position angles of the major axes for the bulge and disk is given in the ninth column of Table 2. (Note that $\Delta P.A.$ in the table is only the model-averaged difference of the position angles. In practice, the position angles of the major axes for the disks and bulges exhibit noticeable variations for a number of galaxies.) The last three columns give the galaxy absolute magnitude, its color index, and the bulge-to-total luminosity ratio. The surface brightnesses, absolute magnitudes, and color indices in Table 2 were corrected for the foreground extinction in the Milky Way according to Schlafly and Finkbeiner (2011).

3. Results and discussion

3.1. General characteristics of the galaxies

The integrated characteristics of the polar-bulge galaxies in the r band are as follows: the mean absolute magnitude $\langle M \rangle = -19.9 \pm 0.7$, the mean color index $\langle g - r \rangle = 0.64 \pm 0.16$, and the exponential scale length of the disk $\langle h \rangle = 5.1 \pm 1.0$ kpc. In all these characteristics, our objects are typical bright spiral galaxies of late morphological types (see, e.g., Bizyaev et al. 2014). The mean vertical scale height of the stellar disk in the r band, $\langle z_0 \rangle = 1.50 \pm 0.54$ kpc, is also near the peak of the distribution for the galaxies from the EGIS catalog. If we exclude the two galaxies (#3 and #6 in Table 1) whose inclination visually deviates most strongly from 90° , then this value decreases to $\langle z_0 \rangle = 1.36 \pm 0.45$ kpc.

The mean relative disk thickness for the galaxies of our sample is $\langle z_0/h \rangle = 0.285 \pm 0.07$; without galaxies #3 and #6, it is $\langle z_0/h \rangle = 0.265 \pm 0.06$. These values are close to the galactic disk thickness in well-defined samples of edge-on spiral galaxies (Mosenkov et al. 2015).

The mean ratio of the disk exponential scale length in the g and r bands for the considered sample is 1.09 ± 0.10 , which implies the existence of a color gradient: the galactic disks become bluer towards the

Table 2. Photometric characteristics of the galaxies in the r band

N	μ_e	r_e ($''$)	n	q	μ_0	h ($''$)	z_0 ($''$)	$\Delta P.A.$ ($^\circ$)	M_r	$g-r$	B/T
1	22.57 0.33	2.17 0.32	6.84 2.40	0.85 0.04	22.16 0.10	4.25 0.17	0.88 0.06	73.0 3.6	-20.51	0.75	0.80
2	22.03 0.44	2.73 0.49	1.82 2.23	0.87 0.10	20.93 0.23	5.09 0.32	1.21 0.15	74.7 10.3	-19.85	1.02	0.36
3	21.46 0.17	2.17 0.15	5.44 0.86	0.69 0.03	21.22 0.02	6.37 0.07	2.77 0.03	71.3 1.8	-20.86	0.56	0.36
4	21.94 0.03	2.55 0.03	0.39 0.02	0.47 0.01	21.31 0.01	6.48 0.06	1.60 0.02	89.5 0.6		0.58	0.18
5	21.38 0.04	4.12 0.06	2.53 0.16	0.42 0.02	21.39 0.01	12.00 0.09	3.10 0.02	72.2 0.4	-20.07	0.57	0.36
6	20.19 0.13	1.41 0.07	1.50 0.08	0.66 0.02	22.47 0.06	8.22 0.37	2.43 0.29	49.8 3.2	-19.09	0.44	0.56
7	20.89 0.01	5.95 0.04	0.86 0.02	0.80 0.01	21.61 0.01	23.67 0.08	5.43 0.02	89.7 0.1	-18.75	0.64	0.44
8	21.40 0.06	3.04 0.08	4.13 0.48	0.42 0.03	21.88 0.03	8.28 0.16	2.97 0.02	39.1 0.7	-20.09	0.65	0.47
9	22.07 0.36	2.69 0.23	0.72 0.08	0.68 0.03	21.37 0.08	7.54 0.21	2.25 0.12	87.4 6.7	-20.12	0.57	0.20

periphery. This feature is typical for most of spiral galaxies.

An interesting structural peculiarity of the galaxies in our sample is that their disks exhibit prominent integral-shaped warps (see Fig. 1) in approximately half of the cases. Since the warp is easier to detect in the case where its line of nodes is close to the line of sight, it can be concluded that the stellar disks in most of the polar-bulge galaxies are warped. Strong optical warps are observed in galaxies relatively rarely. As a rule, their existence is associated with the gravitational interaction of galaxies and external accretion (Reshetnikov and Combes 1998, 1999; Ann and Park 2006).

We did not specially study the spatial environment of the galaxies from our sample, but a simple analysis of the SDSS images (in particular, deeper images from Stripe 82 are available for galaxy 1 from our list; Abazajian et al. 2009) showed that relatively close galaxies of comparable luminosity and a number of fainter companions are observed near most of the objects (six out of nine). Unfortunately, there are no available redshifts for the neighboring galaxies, which does not allow us to decide about their spatial association with our objects.

More reliable data are available for previously known galaxies with decoupled bulges. UGC 10043 (#7 in Table 1) is a member of a group, and it inter-

acts with the galaxy MCG+04-37-035 (Aguirre et al. 2009). Two other galaxies (NGC 4672 and NGC 4698; see Introduction) are not isolated either. NGC 4672 is a member of a group of galaxies (Garcia 1993); NGC 4698 is a member of the Virgo cluster of galaxies.

3.2. Photometric characteristics of bulges

The distributions of the main characteristics of the decoupled bulges in the r band are shown in Fig. 2. By comparing these distributions with the characteristics of the central objects in polar-ring galaxies (Fig. 2 in Reshetnikov and Combes 2015) it can be noted that, as expected, the bulges are more compact and faint, on average. For example, the mean absolute r -band magnitude for the bulges of our sample is $\langle M \rangle = -18.95 \pm 0.77$ (compare with -20.34 for the centers of the polar-ring galaxies), while the mean effective radius in the same band is $\langle r_e \rangle = 1.86 \pm 0.74$ kpc (3.2 kpc for polar-ring galaxies). The distribution of the Sersic index for the bulges appears almost flat (Fig. 2b) and does not show a distinct peak typical for the bulges of spiral galaxies of early morphological types (Tasca and White 2011). In general, the observed distribution is close to that for the bulges of the late-type spiral galaxies, with caution from the limited size of our sample.

The mean color index of the decoupled bulges, $\langle g-r \rangle = 0.88 \pm 0.13$, is considerably redder than that

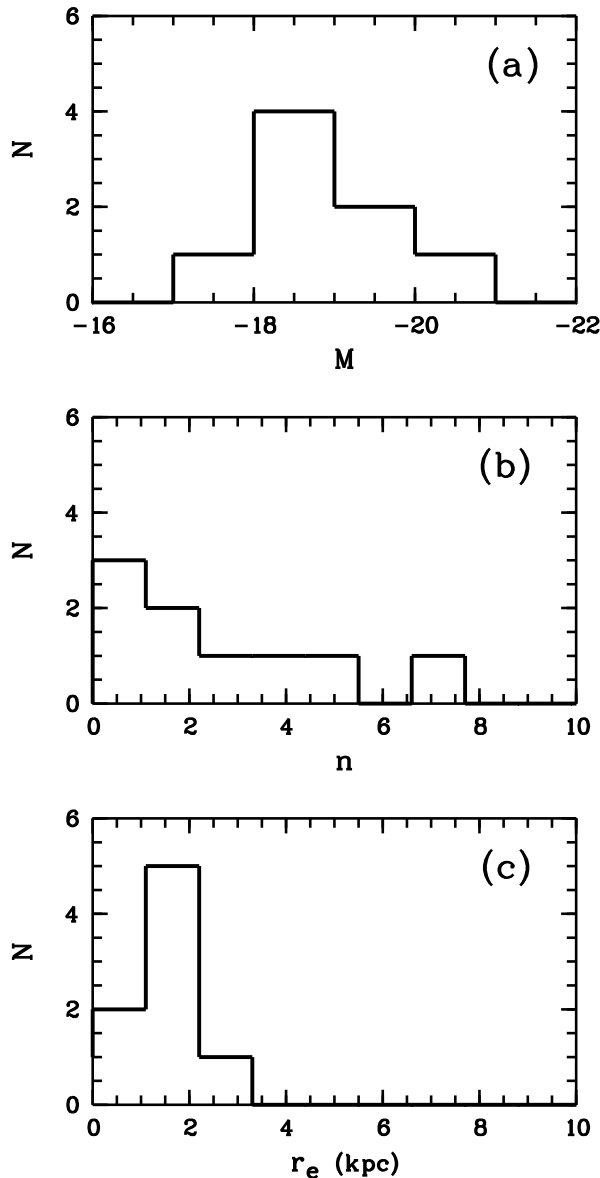


Fig. 2. Observed distributions of the polar-bulge characteristics in the r band: the absolute magnitudes (a), Sersic index (b), and effective radius (c).

of the surrounding disks, for which $\langle g-r \rangle = 0.49 \pm 0.22$. Given that the colors of the edge-on disks were not corrected for the internal extinction, the color difference between the bulges and disks must be even greater. This large color difference between the bulges and disks is typical for galaxies of late morphological types (Mollenhoff 2004).

Fig. 3 shows the photometric scaling relations for the bulges. The relation between the luminosity of morphologically decoupled bulges and their Sersic index is displayed in Fig. 3a. The dashed line in Fig. 3 corresponds to mean relation for the bulges of almost

1000 galaxies constructed from the data of Gadotti (2009) (see Eq. (25) and Fig. 17 in Mosenkov et al. (2014)). As it can be seen from Fig. 3a, the bulges we consider roughly follow the trend typical for the regular galaxies.

Fig. 3b illustrates the luminosity – size relation for the decoupled bulges in the comparison with the mean relation for the bulges plotted from the data of Gadotti (2009) (Eq. (31) in Mosenkov et al. (2014)). The polar bulges follow the relation drawn for the regular bulges, with a slight shift towards the larger sizes. It is difficult to judge the significance of this shift because our sample is small and in addition, the normal bulges show a large scatter on the luminosity – size diagram.

The position of the bulges in the Kormendy relation are shown in Fig. 3c. The bulges are located on this plane approximately along the canonical relation for the E/S0 galaxies with a shift from it and from the central polar-ring galaxies towards the smaller size and down to the lower central brightness. There are faint early-type galaxies and bulges (Capaccioli et al. 1992) in this region (approximately at $\log r_e \leq 0.5$). The polar bulges are at the edge of the region where the polar-ring galaxies are located and are comparable in their characteristics to the faintest and smallest host objects in the polar rings (Fig. 3c).

4. Conclusions

We presented a sample of nine edge-on spiral galaxies whose bulges were decoupled from their disks in the sense that the major axes of the bulges are highly inclined to the disk midplane. Note that we selected the objects based on a purely morphological analysis; therefore, there can be chance projections of two galaxies among our objects. The galaxies with such decoupled, or polar, bulges are extremely rare. Based on the number of galaxies we examined when searching for the polar bulges, we can roughly estimate their relative fraction among the spiral galaxies as $\sim 10^{-3}$.

Our analysis of the photometric characteristics for the galactic disks in the polar-bulge galaxies showed them to be similar to the disks of ordinary late-type (Sc–Sd) spiral galaxies. If we disregard the elongation along the minor axes of the galaxies, the bulges also appear quite typical. The polar bulges are similar to the faintest and smallest of the central galaxies in the polar-ring galaxies.

The peculiarity of the polar-bulge galaxies is that galaxies with strong stellar disk warps are encoun-

tered relatively frequently among them. Since the warp is often interpreted as a consequence of an external perturbation and external accretion, these factors may also be responsible for the formation of polar bulges. As has been noted in Introduction, kinematically decoupled subsystems rotating almost orthogonally to the galactic disks are observed in two out of three previously studied polar bulges. The existence of such subsystems is usually associated with the external accretion. Consequently, the detection of such kinematically decoupled structures in the polar bulges of other galaxies would give a good argument for the hypothesis of the formation of decoupled bulges under external accretion.

However, the question of what is the secondary structure in the polar-bulge galaxies, their disks or bulges, remains unclear. Their similarity to the polar-ring galaxies, where the formation of polar disks/rings is well reproduced in the models with the external accretion from another galaxy or from a cloud of intergalactic gas (Reshetnikov and Sotnikova 1997; Bournaud and Combes 2003; Maccio et al. 2006), may suggest that it is the disk in such objects that is secondary. From this viewpoint, the polar-bulge galaxies are simply the polar-ring galaxies with faint central galaxies. On the other hand, as was discussed by Matthews and de Grijs (2004), the opposite scenario, whereby a pre-existing spiral galaxy captures a small elliptical galaxy in the polar plane to become its bulge, is also possible. Less exotic scenarios can also be considered. In general, it is clear that new observing data and realistic numerical simulations are necessary to clarify the nature of these unique objects.

Acknowledgments

This study was financially supported by the Russian Foundation for Basic Research (project nos. 14-02-810 and 13-02-00416). DB is supported by grant RSCF-14-22-00041.

REFERENCES

1. K.N. Abazajian, J.K. Adelman-McCarthy, M.A. Agueros, et al., *Astrophys. J. Suppl. Ser.* 182, 543 (2015).
2. P. Aguirre, J.M. Uson, and L.D. Matthews, *Rev. Mex. Astron. Astrofis.* 35, 201 (2009).
3. S. Alam, F.D. Albareti, C.A. Prieto, F. Anders, F.S. Anderson, T. Anderton, B.H. Andrews, E. Armengaut, et al., *Astrophys. J. Suppl. Ser.* 219, 12A (2015).
4. H.B. Ann and J.-C. Park, *New Astron.* 11, 293 (2006).
5. P.N. Appleton and C. Struck-Marcell, *Fundam. Cosm. Phys.* 16, 111 (1996).
6. E. Athanassoula, *Mon. Not. R. Astron. Soc.* 358, 1477 (2005).
7. K. Bekki, *Astrophys. J.* 499, 635 (1998).
8. F. Bertola, E.M. Corsini, J.C. Vega Beltran, A. Pizzella, M. Sarzi, M. Cappellari, and S.J. Funes, *Astrophys. J.* 519, L127 (1999).
9. D.V. Bizyaev, S.J. Kautsch, A.V. Mosenkov, V.P. Reshetnikov, N.Ya. Sotnikova, N.V. Yablokova, and R.W. Hillyer, *Astrophys. J.* 787, ID 24 (2014).
10. F. Bournaud and F. Combes, *Astron. Astrophys.* 401, 817 (2003).
11. M. Capaccioli, N. Caon, and M. D’Onofrio, *Mon. Not. R. Astron. Soc.* 259, 323 (1992).
12. E.M. Corsini, J. Méndez-Abreu, N. Pastorello, E. dalla Bonta, L. Morelli, A. Beifiori, A. Pizzella, and F. Bertola, *Mon. Not. R. Astron. Soc.* 423, L79 (2012).
13. P. Erwin, *Astrophys. J.* 799, id. 226 (2015).
14. P. Erwin, R.P. Saglia, M. Fabricius, J. Thomas, N. Nowak, S. Rusli, R. Bender, J.C. Vega Beltran, and J.E. Beckman, *Mon. Not. R. Astron. Soc.* 446, 4039 (2015).
15. D.A. Gadotti, *Mon. Not. R. Astron. Soc.* 393, 1531 (2009).
16. A.M. Garcia, *Astron. Astrophys. Suppl. Ser.* 100, 47 (1993).
17. R.C.W. Houghton, R.L. Davies, E. dalla Bonita, and R. Masters, *Mon. Not. R. Astron. Soc.* 423, 256 (2012).
18. J. Kormendy, *Galactic Bulges*, Ed. by E. Laurikainen, R.F. Peletier, and D.A. Gadotti (Springer, New York, 2015).
19. J. Kormendy and R.C. Kennicutt, *Ann. Rev. Astron. Astrophys.* 42, 603 (2004).
20. P.C. van der Kruit and L. Searl, *Astron. Astrophys.* 95, 105 (1981).
21. A.V. Maccio, B. Moore, and J. Stadel, *Astrophys. J.* 636, L25 (2006).
22. I. Martín-Navarro, J. Bakos, I. Trujillo, J.H. Knapen, E. Athanassoula, A. Bosma, S. Comeron, B.G. Elmegreen, et al., *Mon. Not. R. Astron. Soc.* 427, 1102 (2012).
23. L.D. Matthews and R. de Grijs, *Astron. J.* 128, 137 (2004).

24. J. Méndez-Abreu, *Galactic Bulges*, Ed. by E. Laurikainen, R.F. Peletier, and D.A. Gadotti (Springer, New York, 2015).

25. A.F.J. Moffat, *Astron. Astrophys.* 3, 455 (1969).

26. A.V. Moiseev, K.I. Smirnova, A.A. Smirnova, and V.P. Reshetnikov, *Mon. Not. R. Astron. Soc.* 418, 244 (2011).

27. C. Mollenhoff, *Astron. Astrophys.* 415, 63 (2004).

28. A.V. Mosenkov, N.Ya. Sotnikova, and V.P. Reshetnikov, *Mon. Not. R. Astron. Soc.* 441, 1066 (2014).

29. A.V. Mosenkov, N.Ya. Sotnikova, V.P. Reshetnikov, D.V. Bizyaev, and S.J. Kautsch, *Mon. Not. R. Astron. Soc.* 451, 2376 (2015).

30. Ch.Y. Peng, L.C. Ho, Ch.D. Impey, and H.-W. Rix, *Astron. J.* 139, 2097 (2010).

31. A. Renzini, *The Formation of Galactic Bulges*, Ed. by C.M. Carollo, H.C. Ferguson, and R.F.G. Wyse (Cambridge Univ. Press, Cambridge, 1999).

32. V. Reshetnikov and F. Combes, *Astron. Astrophys.* 337, 9 (1998).

33. V. Reshetnikov and F. Combes, *Astron. Astrophys. Suppl. Ser.* 138, 101 (1999).

34. V. Reshetnikov and F. Combes, *Mon. Not. R. Astron. Soc.* 447, 2287 (2015).

35. V. Reshetnikov and N. Sotnikova, *Astron. Astrophys.* 325, 933 (1997).

36. M. Sarzi, E.M. Corsini, A. Pizzella, J.C. Vega Beltran, M. Cappellari, J.G. Funes, and F. Bertola, *Astron. Astrophys.* 360, 439 (2000).

37. E.F. Schlafly and D.P. Finkbeiner, *Astrophys. J.* 737, ID 103 (2011).

38. J.L. Sersic, *Bol. Asoc. Argentina Astron.* 6, 41 (1963).

39. L.A.M. Tasca and S.D.M. White, *Astron. Astrophys.* 530, A106 (2011).

40. I. Trujillo, J.A.L. Aguerri, J. Cepa, and C.M. Gutierrez, *Mon. Not. R. Astron. Soc.* 328, 977 (2001).

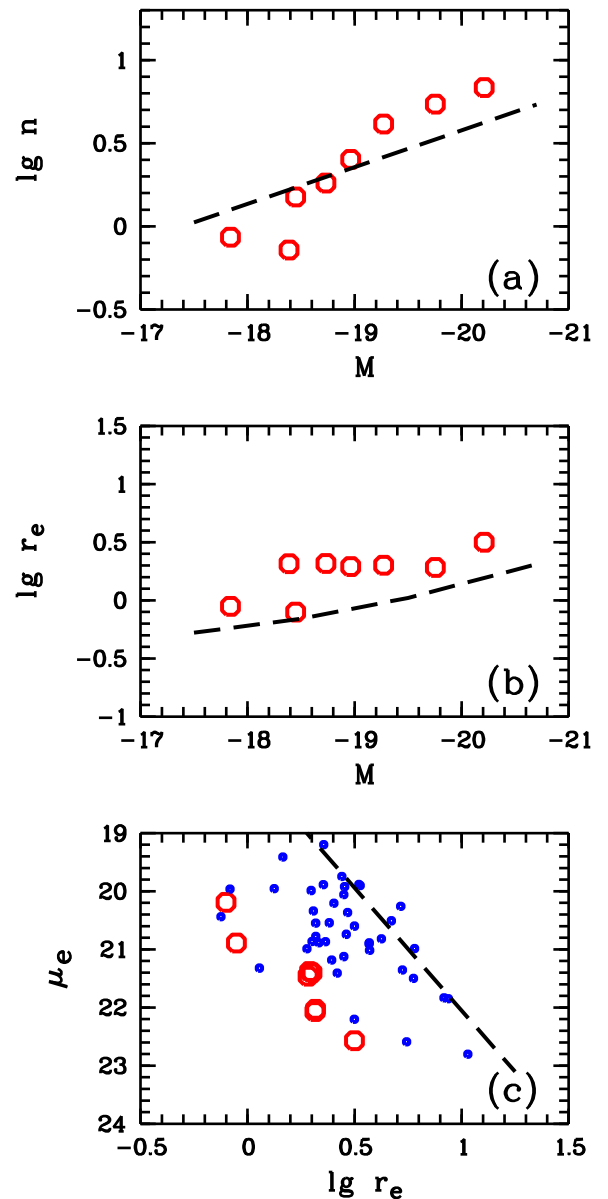


Fig. 3. The scaling relations for the polar bulges in the r band (circles). (a) The luminosity vs Sersic index relation; the dashed line indicates the mean relation for the bulges of regular galaxies (see text). (b) The luminosity vs effective radius (in kpc) relation; the mean relation for normal bulges is indicated by the dashed line. (c) The Kormendy relation; the dashed line indicates the relation for the E/S0 galaxies in the Coma cluster (Houghton et al. 2012); the dots are the characteristics of the polar-ring central galaxies (Reshetnikov and Combes 2015).